

Linear Transceiver Design for Multi-Carrier Full-Duplex MIMO Decode and Forward Relaying

Vimal Radhakrishnan, Omid Taghizadeh, Rudolf Mathar

Institute for Theoretical Information Technology, RWTH Aachen University, D-52056 Aachen, Germany

{radhakrishnan, taghizadeh, mathar}@ti.rwth-aachen.de

Abstract—In this paper, we discuss the linear precoding and decoding design problem for a multi-carrier (MC) full-duplex (FD) decode-and-forward (DF) relaying system. We consider the effects of hardware distortions, which contribute to residual self-interference and also inter-carrier leakage. The impact of the imperfect channel estimation is also taken into account. The problem of linear precoding and decoding design is then studied with the goal of maximizing the system sum rate, leading into a non-convex optimization problem. In addition to the traditional per-carrier DF relaying, the case with a joint subcarrier DF is also studied, taking advantage from a group-wise decoding and encoding. An alternating quadratic convex program (AQCP) is then proposed in each case, with a monotonic improvement at each iteration, leading to a guaranteed convergence. Numerical simulations show a significant gain in terms of the end-to-end system sum rate, in particular when the hardware distortions increase and inter-carrier leakage becomes a dominant factor.

Index Terms—full duplex, decode and forward, relaying, precoding, inter-carrier leakage, hardware distortion, multi-carrier

I. INTRODUCTION

With almost all of the sub 6 GHz spectrum already assigned, combined with the expected 1000-fold increase in the information traffic, spectrum scarcity has been raised as a major problem in future wireless communication systems. In conventional communication systems, the nodes either transmit or receive at the same time-frequency channel resource. In contrast, FD nodes are allowed to transmit and receive simultaneously over the same frequency, thereby showing potential to enhance the spectral efficiency [1]. However, FD nodes suffer from inherent self-interference from their own transmitter. An FD node receives a part of its own transmitted signal through the direct path (LOS) or reflections from the scatterers. Recently, efficient self-interference cancellation (SIC) techniques are developed [2]–[4], which has made feasible to incorporate FD nodes into the future communication systems [5], [6], and motivated some related studies [7], [8]. Most SIC techniques work in both analog and digital domains to remove the self-interference. The major part of the self-interference is removed at the analog domain and the remaining signal will be cancelled in digital domain. In practical scenarios, the SIC level that can be attained depends on various constraints such as inaccurate estimation of interference path, ageing and inaccuracy of hardware components. Hence, it is essential to consider the impact of such inaccuracies, for the purposes of performance evaluation and design of the communication systems benefiting from FD capability.

Full duplex relay systems have also received recognition as it is one of the cost-effective solutions for throughput enhancement, system reliability, energy savings and coverage extension. In [9], the authors have proposed a design strategy for a multi-user FD DF relaying system to overcome its own loopback self-interference, and also provide solution to the case with erroneous CSI following the worst-case enhancement approach. Simultaneous wireless information and power transfer (SWIPT) for a DF FD relay network is investigated in [10]. The outage probability has been derived for multi-hop FD relaying in [11], for orthogonal frequency division multiplexing (OFDM) FD relaying systems in [12], and for FD DF two-way relay systems in [13]. In [14], the authors consider the FD MIMO orthogonal frequency division multiple access (OFDMA) DF relay networks and derive the optimal structure of both source precoding matrix as well as the relay amplifying matrix such that the overall transmission power from source and relay is minimized subject to a given set of QoS constraints. In the aforementioned works, the hardware inaccuracy or hardware distortions are not taken into account.

In [15], the authors have proposed a transmission scheme based on maximization of the lower bound on the end-to-end achievable rate of DF based FD MIMO relay systems under limited dynamic range. Whereas in [16], a convergent block coordinate ascent (BCA) algorithm is developed for maximization of end-to-end achievable rate of the same system. The outage analysis of an FD DF relaying with limited dynamic range of ADC is studied in [17]. The authors have derived the optimal transmit power of the relay to minimize the outage probability. In the above-mentioned works, the authors consider the impact of hardware distortions for a single carrier system.

In this paper, we study an FD MC MIMO DF relaying system, where the effect of hardware distortions, inter carrier leakage and imperfect CSI are jointly taken into account. In Section II, we model the operation of the FD MC MIMO relaying system. We also formulate the impact of hardware inaccuracy with regard to the intended transmit/received signal as well as impact of imperfect CSI. In Section III, we propose an AQCP to maximize the system sum rate, which results in a monotonic improvement thereby leading to a necessary convergence. Moreover, we extend the traditional per-carrier decoding into a joint MC DF scheme, where the information decoded in one subcarrier can be forwarded via another subcarrier. In Section IV, the performance of the proposed

designs are evaluated and compared to the available designs in the literature. It is observed that a significant gain is obtained, via the application of the proposed distortion-aware designs, when transceiver inaccuracy increases and inter-carrier leakage becomes a dominant factor. The main results of this paper are summarized in Section V.

A. Mathematical Notation

Throughout this paper, we denote the vectors and matrices by lower-case and upper-case bold letters, respectively. We use $\mathbb{E}\{\cdot\}$, $|\cdot|$, $\text{tr}(\cdot)$, $(\cdot)^{-1}$, $(\cdot)^*$, $(\cdot)^T$, and $(\cdot)^H$ for mathematical expectation, determinant, trace, inverse, conjugate, transpose, and Hermitian transpose, respectively. We use $\text{diag}(\cdot)$ for the diag operator, which returns a diagonal matrix by setting off-diagonal elements to zero. We denote an all zero matrix of size $m \times n$ by $\mathbf{0}_{m \times n}$. We represent the Euclidean norm as $\|\cdot\|_2$. We denote the set of real, positive real, and complex numbers as \mathbb{R} , \mathbb{R}^+ , and \mathbb{C} respectively.

II. SYSTEM MODEL

Consider an FD MIMO MC DF relaying system with half-duplex (HD) MIMO MC source and destination nodes. The number of transmit antennas at source and relay is denoted as N_s and N_r , respectively, whereas M_r and M_d represent the number of receive antennas at the relay and the destination nodes. The communication between the source and destination is a two-phase communication. In the first phase, the source transmits signals to the relay through the channel $\mathbf{H}_{sr}^k \in \mathbb{C}^{M_r \times N_s}$ with subcarrier $k \in \mathbb{K}$, where $\mathbb{K} := \{1, 2, \dots, K\}$. The received signal from the source is then decoded at the relay after applying self-interference cancellation. In the second phase, the decoded signal at the relay is transmitted to destination through the channel $\mathbf{H}_{rd}^k \in \mathbb{C}^{M_d \times N_r}$, and a part of it is received by the relay itself through the self-interference channel $\mathbf{H}_{rr}^k \in \mathbb{C}^{M_r \times N_r}$. The destination also receives a weak signal (due to path loss) from the source through the direct channel $\mathbf{H}_{sd}^k \in \mathbb{C}^{M_d \times N_s}$, which is considered as an interference, similar to [15], [18]. All channels are constant for each frame, and frequency-flat in each subcarrier, where only imperfect CSI is known. We decompose the true channel into the estimated channel plus some estimation error,

$$\mathbf{H}_{\mathcal{X}} = \hat{\mathbf{H}}_{\mathcal{X}} + \tilde{\mathbf{H}}_{\mathcal{X}}, \quad \hat{\mathbf{H}}_{\mathcal{X}} \perp \tilde{\mathbf{H}}_{\mathcal{X}}, \quad \tilde{\mathbf{H}}_{\mathcal{X}} = \mathbf{D}_{\mathcal{X}}^{\frac{1}{2}} \Delta_{\mathcal{X}}, \quad (1)$$

where $\mathcal{X} \in \{sr, rd, rr, sd\}$, $\hat{\mathbf{H}}_{\mathcal{X}}$ represents the estimated channel, and the entries of $\Delta_{\mathcal{X}}$ are i.i.d complex Gaussian with zero mean and variance one. $\mathbf{D}_{\mathcal{X}}$ shapes the spatial covariance matrix of the CSI estimation error.

A. Source to relay

The transmitted signal from the source can be written as

$$\mathbf{x}_s^k = \underbrace{\mathbf{V}_s^k \mathbf{s}_s^k}_{=:\mathbf{v}_s^k} + \mathbf{e}_{t,s}^k, \quad (2)$$

where $\mathbf{s}_s^k \in \mathbb{C}^{d_s}$, $\mathbf{V}_s^k \in \mathbb{C}^{N_s \times d_s}$, and $\mathbf{e}_{t,s}^k \in \mathbb{C}^{N_s}$ represent the data symbol, the transmit precoding matrix, and transmitter

distortion at the source, respectively. The number of data streams in each subcarrier from the source is denoted by d_s and $\mathbb{E}\{\mathbf{s}_s^k \mathbf{s}_s^{kH}\} = \mathbf{I}_{d_s}$. Furthermore, \mathbf{v}_s^k represents the desired signal to be transmitted from the source. Accordingly, the received signal at the relay can be written as

$$\mathbf{y}_r^k = \underbrace{\mathbf{H}_{sr}^k \mathbf{x}_s^k + \mathbf{H}_{rr}^k \mathbf{x}_r^k}_{=:\mathbf{u}_r^k} + \mathbf{n}_r^k + \mathbf{e}_{r,r}^k, \quad (3)$$

where $\mathbf{n}_r^k \sim \mathcal{CN}(\mathbf{0}_{M_r}, \sigma_{r,k}^2 \mathbf{I}_{M_r})$ and $\mathbf{e}_{r,r}^k$ are the noise and receiver distortion at the relay, respectively. Moreover, \mathbf{u}_r^k represents the intended (distortion-free) signal to be received at the relay. The distortion-free (known) part of the self-interference can be removed via applying an SIC technique [4], [8]. The received signal after SIC can be stated as

$$\tilde{\mathbf{y}}_r^k = \mathbf{y}_r^k - \hat{\mathbf{H}}_{rr}^k \mathbf{V}_r^k \mathbf{s}_r^k = \mathbf{H}_{sr}^k \mathbf{V}_s^k \mathbf{s}_s^k + \mathbf{v}_r^k, \quad (4)$$

where \mathbf{s}_r^k is the decoded signal at the relay and the collective interference-plus-noise at the relay is

$$\mathbf{v}_r^k = \mathbf{H}_{sr}^k \mathbf{e}_{t,s}^k + \tilde{\mathbf{H}}_{rr}^k \mathbf{V}_r^k \mathbf{s}_r^k + \mathbf{H}_{rr}^k \mathbf{e}_{t,r}^k + \mathbf{n}_r^k + \mathbf{e}_{r,r}^k. \quad (5)$$

The estimated signal vector at the relay can be obtained as

$$\tilde{\mathbf{s}}_s^k = (\mathbf{U}_r^k)^H \tilde{\mathbf{y}}_r^k, \quad (6)$$

where \mathbf{U}_r^k represents the linear receive filter at the relay.

B. Relay to destination

The transmitted signal from the relay can be written as

$$\mathbf{x}_r^k = \underbrace{\mathbf{V}_r^k \mathbf{s}_r^k}_{=:\mathbf{v}_r^k} + \mathbf{e}_{t,r}^k, \quad (7)$$

where $\mathbf{V}_r^k \in \mathbb{C}^{N_r \times d_r}$ and $\mathbf{e}_{t,r}^k \in \mathbb{C}^{N_r}$ represent the transmit precoding matrix and transmitter distortion at the relay, respectively. The number of data streams in each subcarrier from the relay is denoted by d_r and $\mathbb{E}\{\mathbf{s}_r^k \mathbf{s}_r^{kH}\} = \mathbf{I}_{d_r}$. Moreover, \mathbf{v}_r^k represents the desired signal to be transmitted from the relay. Consequently, the signal received at the destination including the interference from the source can be written as

$$\begin{aligned} \mathbf{y}_d^k &= \underbrace{\mathbf{H}_{rd}^k \mathbf{x}_r^k + \mathbf{H}_{sd}^k \mathbf{x}_s^k}_{=:\mathbf{u}_d^k} + \mathbf{n}_d^k + \mathbf{e}_{r,d}^k \\ &= \mathbf{H}_{rd}^k \mathbf{V}_r^k \mathbf{s}_r^k + \mathbf{H}_{rd}^k \mathbf{e}_{t,r}^k + \mathbf{H}_{sd}^k \mathbf{V}_s^k \mathbf{s}_s^k + \mathbf{H}_{sd}^k \mathbf{e}_{t,s}^k \\ &\quad + \mathbf{e}_{r,d}^k + \mathbf{n}_d^k, \end{aligned} \quad (8)$$

where $\mathbf{n}_d^k \sim \mathcal{CN}(\mathbf{0}_{M_d}, \sigma_{d,k}^2 \mathbf{I}_{M_d})$ and $\mathbf{e}_{r,d}^k$ are the noise and receiver distortion at the destination. Furthermore, \mathbf{u}_d^k represents the intended (distortion-free) signal to be received at the destination. The direct link is considered as an interference at the destination as its signal power is very weak (due to path loss). Accordingly, the collective interference-plus-noise at the destination can be stated as

$$\mathbf{v}_d^k = \mathbf{H}_{rd}^k \mathbf{e}_{t,r}^k + \mathbf{H}_{sd}^k \mathbf{V}_s^k \mathbf{s}_s^k + \mathbf{H}_{sd}^k \mathbf{e}_{t,s}^k + \mathbf{e}_{r,d}^k + \mathbf{n}_d^k. \quad (9)$$

The estimated signal vector at the destination can be obtained as

$$\tilde{\mathbf{s}}_r^k = (\mathbf{U}_d^k)^H \mathbf{y}_d^k. \quad (10)$$

where \mathbf{U}_r^k is the linear receive filter at the destination.

The mathematical model for the hardware distortions, due to the limited dynamic range of the receiver is, introduced in [19], [20], and utilized in [15]–[17]. We model the transmit and receiver distortions similar to that of [19]. The statistics of the distortion terms can be written as

$$\mathbf{e}_{t,s}^k \sim \mathcal{CN}\left(\mathbf{0}_{N_s}, \frac{B^k}{B_{tot}} \boldsymbol{\Theta}_{tx,s} \mathbf{P}_{tx,s}\right), \quad (11)$$

$$\mathbf{e}_{t,r}^k \sim \mathcal{CN}\left(\mathbf{0}_{N_r}, \frac{B^k}{B_{tot}} \boldsymbol{\Theta}_{tx,r} \mathbf{P}_{tx,r}\right), \quad (12)$$

$$\mathbf{e}_{r,r}^k \sim \mathcal{CN}\left(\mathbf{0}_{M_r}, \frac{B^k}{B_{tot}} \boldsymbol{\Theta}_{tx,r} \mathbf{P}_{rx,r}\right), \quad (13)$$

$$\mathbf{e}_{r,d}^k \sim \mathcal{CN}\left(\mathbf{0}_{M_d}, \frac{B^k}{B_{tot}} \boldsymbol{\Theta}_{rx,d} \mathbf{P}_{rx,d}\right), \quad (14)$$

where

$$\mathbf{P}_{tx,s} := \sum_{k \in \mathbb{K}} \text{diag}\left(\mathbb{E}\{\mathbf{v}_s^k \mathbf{v}_s^{kH}\}\right), \quad (15)$$

$$\mathbf{P}_{tx,r} := \sum_{k \in \mathbb{K}} \text{diag}\left(\mathbb{E}\{\mathbf{v}_r^k \mathbf{v}_r^{kH}\}\right), \quad (16)$$

$$\mathbf{P}_{rx,r} := \sum_{k \in \mathbb{K}} \text{diag}\left(\mathbb{E}\{\mathbf{u}_r^k \mathbf{u}_r^{kH}\}\right), \quad (17)$$

$$\mathbf{P}_{rx,d} := \sum_{k \in \mathbb{K}} \text{diag}\left(\mathbb{E}\{\mathbf{u}_d^k \mathbf{u}_d^{kH}\}\right), \quad (18)$$

where B^k and B_{tot} represent the bandwidth allocated for each subcarrier and the total bandwidth of the system, respectively. $\boldsymbol{\Theta}_{tx,s}$ and $\boldsymbol{\Theta}_{tx,r}$ ($\boldsymbol{\Theta}_{rx,r}$ and $\boldsymbol{\Theta}_{rx,d}$) are diagonal matrices consisting of transmit (receive) distortion coefficients for the corresponding chains. Please refer to [19] for the detailed definition of the used distortion model. Correspondingly, $\mathbf{P}_{tx,s}$ and $\mathbf{P}_{tx,r}$ ($\mathbf{P}_{rx,r}$ and $\mathbf{P}_{rx,d}$) are the diagonal matrices including intended transmit (receive) signal power at the corresponding chains. The covariance of the received collective interference-plus-noise signal at the relay can be hence obtained as

$$\begin{aligned} \boldsymbol{\Sigma}_r^k &= \mathbb{E}\{\boldsymbol{\nu}_r^k \boldsymbol{\nu}_r^{kH}\} \\ &= \mathbf{H}_{sr}^k \boldsymbol{\Theta}_{tx,s}^k \text{diag}\left(\sum_{l \in \mathbb{K}} \mathbf{V}_s^l \mathbf{V}_s^{lH}\right) \mathbf{H}_{sr}^{kH} \\ &+ \mathbf{H}_{rr}^k \boldsymbol{\Theta}_{tx,r}^k \text{diag}\left(\sum_{l \in \mathbb{K}} \mathbf{V}_r^l \mathbf{V}_r^{lH}\right) \mathbf{H}_{rr}^{kH} + \mathbf{D}_{rr} \text{tr}(\mathbf{V}_r^k \mathbf{V}_r^{kH}) \\ &+ \boldsymbol{\Theta}_{rx,r}^k \text{diag}\left(\sum_{l \in \mathbb{K}} \mathbf{H}_{sr}^l \mathbf{V}_s^l \mathbf{V}_s^{lH} \mathbf{H}_{sr}^{lH}\right) \\ &+ \sum_{l \in \mathbb{K}} \mathbf{H}_{rr}^l \mathbf{V}_r^l \mathbf{V}_r^{lH} \mathbf{H}_{rr}^{lH} + \sum_{l \in \mathbb{K}} \sigma_{r,l}^2 \mathbf{I}_{M_r} \\ &+ \sigma_{r,k}^2 \mathbf{I}_{M_r}, \quad k \in \mathbb{K}. \end{aligned} \quad (19)$$

Similarly, the covariance of the interference-plus-noise signal at the destination is obtained as

$$\begin{aligned} \boldsymbol{\Sigma}_d^k &= \mathbb{E}\{\boldsymbol{\nu}_d^k \boldsymbol{\nu}_d^{kH}\} \\ &= \mathbf{H}_{rd}^k \boldsymbol{\Theta}_{tx,r}^k \text{diag}\left(\sum_{l \in \mathbb{K}} \mathbf{V}_r^l \mathbf{V}_r^{lH}\right) \mathbf{H}_{rd}^{kH} \\ &+ \mathbf{H}_{sd}^k \boldsymbol{\Theta}_{tx,s}^k \text{diag}\left(\sum_{l \in \mathbb{K}} \mathbf{V}_s^l \mathbf{V}_s^{lH}\right) \mathbf{H}_{sd}^{kH} \\ &+ \boldsymbol{\Theta}_{rx,d}^k \text{diag}\left(\sum_{l \in \mathbb{K}} \mathbf{H}_{rd}^l \mathbf{V}_r^l \mathbf{V}_r^{lH} \mathbf{H}_{rd}^{lH}\right) \\ &+ \sum_{l \in \mathbb{K}} \mathbf{H}_{sd}^l \mathbf{V}_s^l \mathbf{V}_s^{lH} \mathbf{H}_{sd}^{lH} + \sum_{l \in \mathbb{K}} \sigma_{d,l}^2 \mathbf{I}_{M_d} \\ &+ \sigma_{d,k}^2 \mathbf{I}_{M_d}, \quad k \in \mathbb{K}. \end{aligned} \quad (20)$$

C. Mean-Squared Error (MSE) matrix

Considering \mathbf{V}_s^k and \mathbf{U}_r^k as the linear transmit precoder and receive filters, the MSE matrix for the source-relay system can be defined as

$$\begin{aligned} \mathbf{E}_r^k &= \mathbb{E}\{(\tilde{\mathbf{s}}_s^k - \mathbf{s}_s^k)(\tilde{\mathbf{s}}_s^k - \mathbf{s}_s^k)^H\} \\ &= ((\mathbf{U}_r^k)^H \mathbf{H}_{sr}^k \mathbf{V}_s^k - \mathbf{I}_{d_s}) ((\mathbf{U}_r^k)^H \mathbf{H}_{sr}^k \mathbf{V}_s^k - \mathbf{I}_{d_s})^H \\ &\quad + (\mathbf{U}_r^k)^H \boldsymbol{\Sigma}_r^k \mathbf{U}_r^k. \end{aligned} \quad (21)$$

Similarly, the MSE matrix for the relay-destination system via applying \mathbf{V}_r^k and \mathbf{U}_d^k as the linear transmit precoder and receive filters can be obtained as

$$\begin{aligned} \mathbf{E}_d^k &= \mathbb{E}\{(\tilde{\mathbf{s}}_r^k - \mathbf{s}_r^k)(\tilde{\mathbf{s}}_r^k - \mathbf{s}_r^k)^H\} \\ &= ((\mathbf{U}_d^k)^H \mathbf{H}_{rd}^k \mathbf{V}_r^k - \mathbf{I}_{d_r}) ((\mathbf{U}_d^k)^H \mathbf{H}_{rd}^k \mathbf{V}_r^k - \mathbf{I}_{d_r})^H \\ &\quad + (\mathbf{U}_d^k)^H \boldsymbol{\Sigma}_d^k \mathbf{U}_d^k. \end{aligned} \quad (22)$$

III. SUM RATE MAXIMIZATION

The sum rate maximization problem for the relay system can be presented as

$$\max_{\mathbf{V}_s, \mathbf{U}_r, \mathbf{V}_r, \mathbf{S}_r, \mathbf{U}_d, \mathbf{S}_d} \min\{\mathbf{I}_{sr}, \mathbf{I}_{rd}\} \quad (23a)$$

$$\text{subject to } \text{tr}((\mathbf{I}_{N_s} + \boldsymbol{\Theta}_{tx,s}) \sum_{l \in \mathbb{K}} \mathbf{V}_s^l \mathbf{V}_s^{lH}) \leq P_s, \quad (23b)$$

$$\text{tr}((\mathbf{I}_{N_r} + \boldsymbol{\Theta}_{tx,r}) \sum_{l \in \mathbb{K}} \mathbf{V}_r^l \mathbf{V}_r^{lH}) \leq P_r, \quad (23c)$$

where \mathbf{I}_{sr} and \mathbf{I}_{rd} are total sum rate between the source and relay, and relay and destination, respectively. P_s and P_r denote the maximum affordable transmit power at the source and the relay, respectively. Considering \mathbf{V}_s and \mathbf{V}_r as linear transmit precoders at source and relay, respectively, the rate functions can be defined as

$$\begin{aligned} \mathbf{I}_{sr} &= \sum_{k \in \mathbb{K}} \mathbf{I}_{sr}^k \\ &= \sum_{k \in \mathbb{K}} B^k \log_2 |\mathbf{I}_{d_s} + \mathbf{V}_s^k \mathbf{H}_{sr}^k (\boldsymbol{\Sigma}_r^k)^{-1} \mathbf{H}_{sr}^k \mathbf{V}_s^k| \end{aligned}$$

and

$$\begin{aligned} \mathbf{I}_{rd} &= \sum_{k \in \mathbb{K}} \mathbf{I}_{rd}^k \\ &= \sum_{k \in \mathbb{K}} B^k \log_2 |\mathbf{I}_{dr} + \mathbf{V}_r^k H \mathbf{H}_{rd}^k H (\boldsymbol{\Sigma}_d^k)^{-1} \mathbf{H}_{rd}^k \mathbf{V}_r^k|. \end{aligned}$$

The optimization problem (23) can be reformulated as

$$\begin{aligned} \max_{\mathbf{V}_s, \mathbf{U}_r, \mathbf{V}_r, \mathbf{S}_r, \mathbf{U}_d, \mathbf{S}_d} \quad & \sum_{k \in \mathbb{K}} t_k \\ \text{subject to} \quad & \mathbf{I}_{sr}^k \geq t_k \\ & \mathbf{I}_{rd}^k \geq t_k \end{aligned} \quad (24)$$

(23b), (23c).

It can be observed that the problem (24) is not a convex optimization problem. In the following, we apply the known WMMSE method [21] to facilitate a convergent alternating optimization.

We can write the optimal MMSE receive filter at relay as,

$$\mathbf{U}_{r,mmse}^k = (\boldsymbol{\Sigma}_r^k + \mathbf{H}_{sr}^k \mathbf{V}_s^k \mathbf{V}_s^k H \mathbf{H}_{sr}^k H)^{-1} \mathbf{H}_{sr}^k \mathbf{V}_s^k \quad (25)$$

and at destination as

$$\mathbf{U}_{d,mmse}^k = (\boldsymbol{\Sigma}_d^k + \mathbf{H}_{rd}^k \mathbf{V}_r^k \mathbf{V}_r^k H \mathbf{H}_{rd}^k H)^{-1} \mathbf{H}_{rd}^k \mathbf{V}_r^k. \quad (26)$$

By applying (25) and (26) in (21) and (22), we get,

$$\mathbf{E}_{r,mmse}^k = (\mathbf{I}_{ds} + \mathbf{V}_s^k H \mathbf{H}_{sr}^k H (\boldsymbol{\Sigma}_r^k)^{-1} \mathbf{H}_{sr}^k \mathbf{V}_s^k)^{-1}, \quad (27)$$

$$\mathbf{E}_{d,mmse}^k = (\mathbf{I}_{dr} + \mathbf{V}_r^k H \mathbf{H}_{rd}^k H (\boldsymbol{\Sigma}_d^k)^{-1} \mathbf{H}_{rd}^k \mathbf{V}_r^k)^{-1}. \quad (28)$$

Using (27) and (28), the rate functions can be written as

$$\mathbf{I}_{sr}^k = -B^k \log_2 |\mathbf{E}_{r,mmse}^k|, \quad (29)$$

$$\mathbf{I}_{rd}^k = -B^k \log_2 |\mathbf{E}_{d,mmse}^k|. \quad (30)$$

By using the same reasoning as lemma III.1. of [19], the optimization problem (24) can be written as

$$\max_{\mathbf{V}_s, \mathbf{U}_r, \mathbf{V}_r, \mathbf{S}_r, \mathbf{U}_d, \mathbf{S}_d} \quad \sum_{k \in \mathbb{K}} t_k \quad (31a)$$

$$\text{subject to} \quad B^k (-\text{tr}(\mathbf{S}_r^k \mathbf{E}_r^k) + \log |\mathbf{S}_r^k| + d_s) \geq t_k, \quad (31b)$$

$$B^k (-\text{tr}(\mathbf{S}_d^k \mathbf{E}_d^k) + \log |\mathbf{S}_d^k| + d_r) \geq t_k, \quad (31c)$$

(23b), (23c).

Please note that the obtained problem is not a jointly convex problem. However, it is a quadratic convex program over \mathbf{V}_s and \mathbf{V}_r , when other variables are fixed. Moreover the optimization over \mathbf{U}_r and \mathbf{U}_d can be obtained from (25) and (26), respectively. Whereas, the optimization over \mathbf{S}_r and \mathbf{S}_d can be acquired using (27) and (28), as $\mathbf{S}_r^k = \mathbf{E}_r^k$ and $\mathbf{S}_d^k = \mathbf{E}_d^k$. This facilitates an alternating optimization where each step the corresponding problem is solved to optimality. Due to monotonic increase of the objective in each step and the fact that the system sum rate is bounded from above, the alternating optimization steps lead to convergence. Algorithm 1 defines the detailed algorithm procedure.

Algorithm 1 AQCP-WMMSE design for sum rate maximization

- 1: $a \leftarrow 0$ (set iteration number to zero)
 - 2: $\mathbf{V}_s, \mathbf{V}_r \leftarrow$ right singular matrix initialization [22, Appendix A]
 - 3: **repeat**
 - 4: $a \leftarrow a + 1$
 - 5: $\mathbf{U}_r, \mathbf{U}_d \leftarrow$ solve (25) and (26), respectively
 - 6: $\mathbf{S}_r, \mathbf{S}_d \leftarrow \mathbf{S}_r^k = \mathbf{E}_r^k$ and $\mathbf{S}_d^k = \mathbf{E}_d^k$, respectively
 - 7: $\mathbf{V}_s, \mathbf{V}_r \leftarrow$ solve (31), with fixed $\mathbf{U}_r, \mathbf{U}_d, \mathbf{S}_r$, and \mathbf{S}_d
 - 8: **until** a stable point, or maximum number of a reached
 - 9: **return** $\{\mathbf{V}_s, \mathbf{V}_r\}$
-

A. Joint-Carrier (JC) decoding and remapping

In this section, we consider the optimization constraints over all the subcarriers jointly. It takes advantage of the MC system, by allowing the relay system to decode the signal from one subcarrier and forward it to the destination through another subcarrier, thereby improving the system in terms of total sum rate. Accordingly, the sum rate optimization problem with joint-carrier decoding and remapping can be defined as

$$\begin{aligned} \max_{\mathbf{V}_s, \mathbf{U}_r, \mathbf{V}_r, \mathbf{S}_r, \mathbf{U}_d, \mathbf{S}_d} \quad & t \\ \text{subject to} \quad & \sum_{k \in \mathbb{K}} B^k (-\text{tr}(\mathbf{S}_r^k \mathbf{E}_r^k) + \log |\mathbf{S}_r^k| + d_s) \geq t, \\ & \sum_{k \in \mathbb{K}} B^k (-\text{tr}(\mathbf{S}_d^k \mathbf{E}_d^k) + \log |\mathbf{S}_d^k| + d_r) \geq t, \end{aligned} \quad (32)$$

(23b), (23c).

Similar alternating quadratic convex program steps that are applied to (31) can be used to solve the above optimization problem (32).

IV. SIMULATION RESULTS

In this section, by using numerical simulations, we evaluate the performance of the proposed transceiver design (JC) introduced in subsection III-A for an FD MC MIMO DF relay system. We compare the proposed design with other benchmarks such as, per-carrier (PC) design, where the design maximizes for each sub-carrier individually, less-distortion (LD) design, where the hardware inaccuracy at the source and destination are not taken into account, i.e., only hardware inaccuracy at the relay is considered, no-distortion (ND) design, where hardware inaccuracy is not taken into account [14] and half-duplex (HD) design. All communication channels follow an uncorrelated Rayleigh flat fading model. The self-interference channel follows the characterization reported in [1], i.e., $\mathbf{H}_{rr} \sim \mathcal{CN} \left(\sqrt{\frac{\rho_{si} K_R}{1+K_R}} \mathbf{H}_0, \frac{\rho_{si}}{1+K_R} \mathbf{I}_{M_r} \otimes \mathbf{I}_{N_r} \right)$, where ρ_{si} is the self-interference channel strength, \mathbf{H}_0 is a deterministic matrix of all-1 elements, and K_R is the Rician coefficient. The overall system performance is then averaged over 100 channel realizations. During our simulations, the following values are used to define the default setup: $K = 4$, $K_R = 1$, $N = N_s = M_r = N_r = M_d = 2$, $\rho = \rho_{sr} = \rho_{rd} = -20dB$, $\rho_{sd} = -30dB$, $\rho_{si} = 1$, $\sigma_n^2 = \sigma_{r,k}^2 = \sigma_{d,k}^2 = -30dB$,

$P_{max} = P_s = P_r = 1$, $d = d_s = d_r = 2$, $\kappa = -50\text{dB}$ where $\Theta_{tx,s}^k = \Theta_{tx,r}^k = \kappa \mathbf{I}_N$ and $\Theta_{rx,r}^k = \Theta_{rx,d}^k = \kappa \mathbf{I}_N$. The spatial covariance matrix of the estimated error is assumed to be identity matrix.

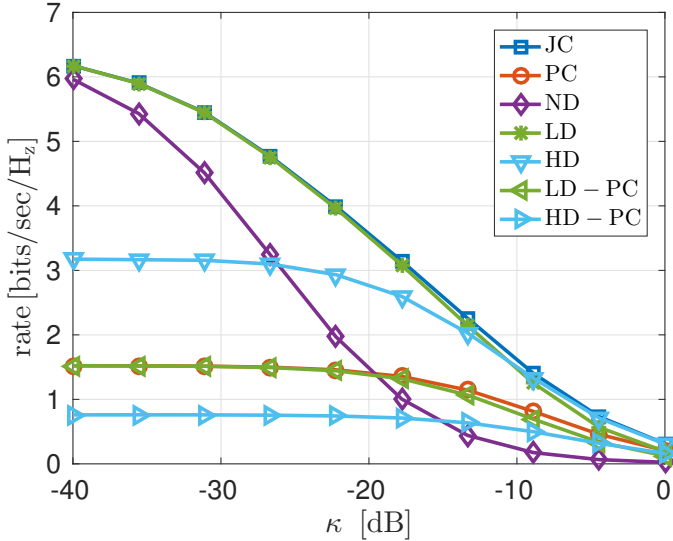


Fig. 1. Sum rate vs. hardware inaccuracy.

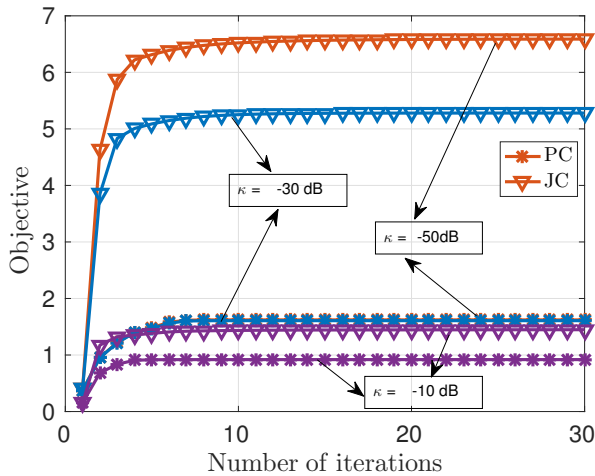


Fig. 2. Average convergence behaviour of JC and PC algorithms.

κ dB	JC	PC	LD	LD - PC	ND
-40	80.32	46.41	53.45	30.59	27.14
-20	63.18	46.15	42.95	30.62	27.18
-5	69.23	50.15	43.93	33.60	27.18

TABLE I

COMPARISON OF COMPUTATIONAL COMPLEXITY IN TERMS OF THE COMPUTATIONAL TIME (SECS).

In Fig. 1, the performance of the design in terms of system sum rate is evaluated for different values of transceiver accuracy. As we can observe, the sum rate decreases as the

transceiver inaccuracy increases, i.e., higher the κ smaller the sum rate. It is clear that the proposed design (JC) outperforms all the other benchmarks. It is interesting to observe that the less distortion (LD) design performs similar to the JC design except for the higher values of κ , which is not very usual in the practical case.

In Fig. 2, the average convergence behaviour is plotted for different values of hardware inaccuracy κ dB. We apply right-singular matrix (RSM) initialization proposed in [22, Appendix A]. It is observed that the algorithm converges within 10-25 iterations. As expected, it can be seen that the objective has higher value for smaller hardware inaccuracy. In spite of the fact that the global optimality of the final solution can not be verified due to the possibility of the local solutions, the numerical simulations exhibit that the algorithm shows a good convergence behaviour when the RSM initialization is applied.

In Table. I, computational complexity of the algorithms in terms of the required computational time (CT) are depicted for different values of transceiver accuracy¹. It can be seen that, the JC design requires a high CT compared to other algorithms. This is due to the consideration of distortion of all the nodes as well as joint subcarrier optimization. It is interesting to observe that LD design performs similar to the JC design with less CT. It also outperforms the PC design even though both designs requires almost similar CT. Hence for complex systems, one can use LD design without significant degradation.

V. CONCLUSIONS

In this paper, we proposed a linear transceiver design for a bidirectional MC FD MIMO DF relaying system taking into account the impact of hardware distortions leading to inter-carrier leakage as well as the impact of CSI error. MC FD systems are usually limited by the residual self-interference, which spreads over multiple carriers (inter-carrier leakage) due to hardware distortion. From our numerical simulations, it can be observed that consideration of hardware distortion is essential as transceiver accuracy reduces. Furthermore, a significant gain can be observed compared to the per-carrier approach and half duplex system. It can also be noticed that the less-distortion approach, which is computationally less complex, performs similar to the proposed design. So for more complex systems such as multiple source-destination scenarios, LD design can be used without significant performance degradation.

REFERENCES

- [1] M. Duarte, C. Dick, and A. Sabharwal, "Experiment-Driven Characterization of Full-Duplex Wireless Systems," *IEEE Transactions on Wireless Communications*, vol. 11, no. 12, pp. 4296–4307, December 2012.
- [2] A. S. E. Everett and A. Sabharwal, "Passive Self-Interference Suppression for Full-Duplex Infrastructure Nodes," *IEEE Transactions on Wireless Communications*, vol. 13, pp. 680–694, 2014.

¹The reported CT is obtained using an Intel Core i7-4790S processor with clock rate of 3.2 GHz and 16 GB RAM. We use MATLAB 2016b on a 64-bit operating system.

- [3] T. Riihonen and R. Wichman, "Analog and digital self-interference cancellation in full-duplex MIMO-OFDM transceivers with limited resolution in A/D conversion," in *2012 Conference Record of the Forty Sixth Asilomar Conference on Signals, Systems and Computers (ASILOMAR)*, Nov 2012, pp. 45–49.
- [4] M. S. Sim, M. Chung, D. Kim, J. Chung, D. K. Kim, and C. Chae, "Nonlinear Self-Interference Cancellation for Full-Duplex Radios: From Link- and System-Level Performance Perspectives," *CoRR*, vol. abs/1607.01912, 2016. [Online]. Available: <http://arxiv.org/abs/1607.01912>
- [5] J. C. M. J. J. M. S. K. P. L. S. Hong, J. Brand, "Applications of self-interference cancellation in 5G and beyond," *IEEE Communications Magazine*, vol. 52, pp. 114–121, 2014.
- [6] R. A. Pitaval, O. Tirkkonen, R. Wichman, K. Pajukoski, E. Lahetkangas, and E. Tirola, "Full-duplex self-backhauling for small-cell 5G networks," *IEEE Wireless Communications*, vol. 22, no. 5, pp. 83–89, October 2015.
- [7] D. Bharadia and S. Katti, "Full Duplex MIMO Radios," in *11th USENIX Symposium on Networked Systems Design and Implementation (NSDI 14)*. Seattle, WA: USENIX Association, 2014, pp. 359–372. [Online]. Available: <https://www.usenix.org/conference/nsdi14/technical-sessions/bharadia>
- [8] A. Sabharwal, P. Schniter, D. Guo, D. W. Bliss, S. Rangarajan, and R. Wichman, "In-Band Full-Duplex Wireless: Challenges and Opportunities," *IEEE Journal on Selected Areas in Communications*, vol. 32, no. 9, pp. 1637–1652, Sept 2014.
- [9] O. Taghizadeh and R. Mathar, "Robust Multi-User Decode-and-Forward Relaying with Full-Duplex Operation," in *The Eleventh International Symposium on Wireless Communication Systems (ISWYS 2014)*, Barcelona, Spain, Sep 2014, pp. 1–7. [Online]. Available: <http://www.ti.rwth-aachen.de/publications/output.php?id=981&table=proceeding&type=pdf>
- [10] H. Liu, K. J. Kim, K. S. Kwak, and H. V. Poor, "Power Splitting-Based SWIPT With Decode-and-Forward Full-Duplex Relaying," *IEEE Transactions on Wireless Communications*, vol. 15, no. 11, pp. 7561–7577, Nov 2016.
- [11] T. K. Baranwal, D. S. Michalopoulos, and R. Schober, "Outage Analysis of Multihop Full Duplex Relaying," *IEEE Communications Letters*, vol. 17, no. 1, pp. 63–66, January 2013.
- [12] S. Wang, W. Yang, and W. Xu, "Outage analysis of OFDM Full Duplex relaying systems," in *2015 International Conference on Wireless Communications Signal Processing (WCSP)*, Oct 2015, pp. 1–4.
- [13] C. Li, Z. Chen, Y. Wang, Y. Yao, and B. Xia, "Outage Analysis of the Full-Duplex Decode-and-Forward Two-Way Relay System," *IEEE Transactions on Vehicular Technology*, vol. 66, no. 5, pp. 4073–4086, May 2017.
- [14] R. Patidar, S. Duwasha, and R. Dubey, "Decode-And-Forward Full Duplex relaying in MIMO-OFDMA Systems," *International journal of innovative research in electrical, electronics, instrumentation and control engineering*, vol. 1, no. 6, September 2013.
- [15] B. P. Day, A. R. Margetts, D. W. Bliss, and P. Schniter, "Full-Duplex MIMO Relaying: Achievable Rates Under Limited Dynamic Range," in *IEEE Journal on Selected Areas in Communications*, 2012.
- [16] H. Shen, C. Liu, W. Xu, and C. Zhao, "Optimized Full-Duplex MIMO DF Relaying With Limited Dynamic Range," *IEEE Access*, vol. 5, pp. 20 726–20 735, 2017.
- [17] J. Ko, M. Jung, and H. Jin, "Outage analysis of full-duplex DF relaying with limited dynamic range of ADC," in *2016 IEEE 27th Annual International Symposium on Personal, Indoor, and Mobile Radio Communications (PIMRC)*, Sept 2016, pp. 1–6.
- [18] O. Taghizadeh, A. Cirik, and R. Mathar, "Hardware Impairments Aware Transceiver Design for Full-Duplex Amplify-and-Forward MIMO Relaying," *IEEE Transactions on Wireless Communications*, vol. PP, no. 99, pp. 1–1, 2017.
- [19] O. Taghizadeh, V. Radhakrishnan, A. C. Cirik, R. Mathar, and L. Lampe, "Linear Transceiver Design for Bidirectional Full-Duplex MIMO OFDM systems," *CoRR*, vol. abs/1704.04815, 2017. [Online]. Available: <http://arxiv.org/abs/1704.04815>
- [20] B. P. Day, D. W. Bliss, A. R. Margetts, and P. Schniter, "Full-duplex bidirectional MIMO: Achievable rates under limited dynamic range," in *2011 Conference Record of the Forty Fifth Asilomar Conference on Signals, Systems and Computers (ASILOMAR)*, Nov 2011, pp. 1386–1390.
- [21] S. S. Christensen, R. Agarwal, E. D. Carvalho, and J. M. Cioffi, "Weighted sum-rate maximization using weighted MMSE for MIMO-BC beamforming design," *IEEE Transactions on Wireless Communications*, vol. 7, no. 12, pp. 4792–4799, December 2008.
- [22] H. Shen, B. Li, M. Tao, and X. Wang, "MSE-Based Transceiver Designs for the MIMO Interference Channel," *IEEE Transactions on Wireless Communications*, vol. 9, no. 11, pp. 3480–3489, November 2010.